Advanced imaging and spectroscopy techniques for body magnetic resonance

Heer, P. de

Cover Page

Universiteit Leiden

The handle http://hdl.handle.net/1887/62452 holds various files of this Leiden University dissertation

Author: Heer, Paul de
Title: Advanced imaging and spectroscopy techniques for body magnetic resonance
Date: 2018-05-23

4

PARAMETER
OPTIMIZATION FOR
REPRODUCIBLE
CARDIAC ^{1}H-MR
SPECTROSCOPY
AT 3 TESLA

4

PARAMETER OPTIMIZATION FOR REPRODUCIBLE CARDIAC [1]H-MR SPECTROSCOPY AT 3 TESLA

Authors
Paul de Heer, MSc,[1] Maurice B. Bizino, MD,[2] Hildo J. Lamb, MD, PhD,[2] and Andrew G. Webb, PhD[1]

[1] C.J. Gorter Center for High Field MRI, Department of Radiology, Leiden University Medical Center, Leiden, the Netherlands.

[2] Department of Radiology, Leiden University Medical Center, Leiden, the Netherlands.

ABSTRACT

Purpose:
To optimize data acquisition parameters in cardiac proton MR spectroscopy, and to evaluate the intra- and intersession variability in myocardial triglyceride content.

Materials and Methods:
Data acquisition parameters at 3 Tesla (T) were optimized and reproducibility measured using, in total, 49 healthy subjects. The signal-to-noise-ratio (SNR) and the variance in metabolite amplitude between averages were measured for: (i) global versus local power optimization; (ii) static magnetic field (B_0) shimming performed during free-breathing or within breathholds; (iii) post R-wave peak measurement times between 50 and 900 ms; (iv) without respiratory compensation, with breathholds and with navigator triggering; and (v) frequency selective excitation, Chemical Shift Selective (CHESS) and Multiply Optimized Insensitive Suppression Train (MOIST) water suppression techniques. Using the optimized parameters intra- and intersession myocardial triglyceride content reproducibility was measured. Two cardiac proton spectra were acquired with the same parameters and compared (intrasession reproducibility) after which the subject was removed from the scanner and placed back in the scanner and a third spectrum was acquired which was compared with the first measurement (intersession reproducibility).

Results:
Local power optimization increased SNR on average by 22% compared with global power optimization (P = 0.0002). The average linewidth was not significantly different for pencil beam B_0 shimming using free-breathing or breathholds (19.1 Hz versus 17.5 Hz; P = 0.15). The highest signal stability occurred at a cardiac trigger delay around 240 ms. The mean amplitude variation was significantly lower for breathholds versus free-breathing (P = 0.03) and for navigator triggering versus free-breathing (P = 0.03) as well as for navigator triggering versus breathhold (P = 0.02). The mean residual water signal using CHESS (1.1%, P = 0.01) or MOIST (0.7%, P = 0.01) water suppression was significantly lower than using frequency selective excitation water suppression (7.0%). Using the optimized parameters an intrasession limits of agreement of the myocardial triglyceride content of −0.11% to +0.04%, and an intersession of −0.15% to +0.9%, were achieved. The coefficient of variation was 5% for the intrasession reproducibility and 6.5% for the intersession reproducibility.

Conclusion:
Using approaches designed to optimize SNR and minimize the variation in inter-average signal intensities and frequencies/phases, a protocol was developed to perform cardiac MR spectroscopy on a clinical 3 T system with high reproducibility.

INTRODUCTION

Cardiac proton MR spectroscopy (MRS) can be used to study the effects of lipid accumulation and lipid toxicity in the heart by means of quantitative measurement of the myocardial triglyceride content (MTGC).[1,2] This value is relevant in patients with metabolic syndrome and type 2 diabetes mellitus (DM2), because higher levels have been linked to an increased risk of heart failure.[3] Because the metabolic syndrome and DM2 can potentially be reversed by therapy or diet, it is important to have a reliable and quantitative way of measuring cardiac lipid accumulation. Currently, the application of MRS is limited to clinical research mainly due to the complexity of the technique in terms of the number of parameters which need to be optimized. These include breathing-motion compensation technique because motion due to breathing introduce dynamic variations in the local static magnetic field leading to an increase in spectral linewidth and decrease in the signal-to-noise ratio (SNR) of the lipid peaks.

Similar effects are seen due to the motion related to the cardiac cycle, deformation of the septum as well as the in- and outflow of blood, therefore, the acquisition must be triggered to the cardiac cycle. Transmit field (B^{1+}) inhomogeneity across the heart leads to under- or overestimation of the tip angle in the myocardial wall if conventional global power optimization routines are used, and subsequently lead to loss in the SNR.[4,5] It has also been shown that the nonuniform flip angle distribution results in sections of the free right ventricular wall and the mid-ventricular and apical septum being obscured.[6,7] The low abundance of lipid protons (generally > 100 times less abundant than water protons) means that many signal averages must be acquired, and a high degree of phase stability between averages is required for optimal SNR.[2,8–11] Because the water signal is much larger than the lipid signal, the water signal needs to be efficiently suppressed to minimize baseline distortions and spurious signals that otherwise complicate metabolite quantification due to vibration induced signal modulations.[12]

The aim of this study is to optimize five of the main parameters and methods used in cardiac proton MRS measurements, namely the method of RF power optimization, B_0 shimming, the measurement point within the cardiac cycle, the method of respiratory motion compensation and the choice of water suppression technique. The choices made also considered the requirement of minimal input from the user to make the overall protocol more robust in order to incorporate it into a clinical scan. Finally, we use these optimized parameters to assess the intra- and intersession reproducibility of cardiac MRS in healthy volunteers.

MATERIALS AND METHODS

Participants

The study was approved by the institutional review board, and written informed consent was obtained from all participants. The study was conducted according to the principles expressed in the Declaration of Helsinki. Forty-nine healthy subjects underwent cardiac MRS between July 2013 and September 2015.

Data Acquisition

Experiments were performed on a 3 Telsa (T) Ingenia whole-body MRI scanner (Philips Healthcare, Best, Netherlands). The body coil was used for transmission and an anterior (16 elements) and a posterior (12 elements) array for reception. The most commonly used sequence in cardiac MRS is point resolved spectroscopy (PRESS)[8,13–16] due to its availability as a standard "product sequence" on commercial platforms, and the fact that it gives twice the SNR of the stimulated echo acquisition method (STEAM) method.[17] Two disadvantages of PRESS localization compared with STEAM are the increased chemical shift displacement and increased minimal echo time.

However, because for this study we were mainly interested in a small chemical shift range of the lipid peaks ($(CH_2)^n$ at 1.3 ppm and CH_3 at 0.9 ppm), this will result in only a minor mismatch in the location of the two metabolites. If both the lipids (1.3 ppm) as well as creatine (3 ppm) are of interest, care should be taken planning the spectroscopy voxel to ensure the creatine still falls within the septum. The water signal (4.7 ppm) used as a reference for the lipid quantification does have a significantly different chemical shift; however, data for non–water-suppressed spectra are acquired with a different transmitter offset, resulting in overlap of the spectroscopic volume of interest (VOI) of the lipid- and water-acquisition. The increased minimal echo time does negate the theoretical double SNR of PRESS localization compared with STEAM; however, this effect is only large when the T^2 of the metabolite of interest low. In a previous study, it has been shown that the use of a high permittivity pads increases the SNR of localized cardiac spectra without affecting spectral linewidth.[18] A similar arrangement was used in this study. A first order pencil beam shimming technique was used to shim the static magnetic field (B_0). This technique requires minimal user input and reconstructs the B_0 distribution in the spectroscopy voxel by capturing multiple (nine) projections.

A 30 s survey and a single breathhold coronal image were acquired to plan the navigator volume. Four-chamber and shortaxis cine images were acquired to plan the MRS voxel in the myocardial interventricular septum. Spectra were recorded using PRESS localization with an echo time (TE) of 35 ms and a repetition time (TR) of 9 s for the non–water-suppressed spectra, and 3.5 s for the water-suppressed spectra to ensure full relaxation of the water and lipid signals. The spectroscopic VOI (15 x 25 x 40 mm^3) was placed in the interventricular septum and pencil beam B_0 shimming was performed on this VOI. The bandwidth of the MRS acquisition was 1500 Hz and 2048 samples were acquired resulting in spectral resolution of 0.73 Hz / sample. Five different parameters were optimized as described below:

Power Optimization.
Spectra were acquired in 15 subjects comparing the standard system "global" power optimization with "local" power optimization. Global in this case refers to the fact that power optimization is performed by integrating the signal intensity over an entire trans-

verse slice through the heart, whereas local applies only to the spectroscopic VOI. It is well-known that there is substantial variation in the transmit (B_1^+) field through the body (and within the heart itself) at 3 T, and so global power optimization is unlikely to result in the correct tip angles within the spectroscopic VOI.[4] Previous studies reported a variation in B_1^+ of 100% over the short axis of the heart.[5-7] Local power optimization method was performed by monitoring the intensity of the water peak and incrementing the tip angles of the excitation pulse and the two refocusing pulses in the PRESS sequence in steps of 5% (range, 90%–150% of the global power optimization result), and choosing the power which produced the maximum signal intensity. The SNR of the water signal was compared for the local and global power optimization using a Wilcoxon signed-rank test.

Comparison of Spectral Linewidth for Freebreathing and Breathhold B_0 Shimming.
First order B_0 pencil beam shimming (nine projections) was performed during freebreathing and in two breathholds of 13 s (max. five projections per breathhold) in eight healthy subjects, after which non–watersuppressed spectra (four averages) were acquired. The full width at half maximum (FWHM) of the water peak was determined for each spectrum and compared using a Wilcoxon signed rank test. To determine the reproducibility of the B_0 shimming, each scan was repeated three times in each subject and the standard deviation determined for these three measurements.

Amplitude Stability as a Function of the Measurement Point within the Cardiac Cycle.
Non–water-suppressed spectra (16 averages) were acquired in three subjects at eight different times (50, 150, 200, 250, 300, 500, 700, and 900 ms) after the peak of the R-wave. The variation of the signal was determined by calculating the standard deviation of the water signal amplitude. The average heart rate was recorded for each subject.

Comparison of Signal Reproducibility Between Freebreathing, Breathhold, and Navigator Triggering.
Non–water-suppressed spectra (16 averages) were acquired in seven subjects with free-breathing, breathholds and navigator triggered respiratory compensation.[13] The breathhold acquisition was performed in eight breathholds of 18 s acquiring two averages per breathhold. The navigator volume was placed on the lung– liver interface and had a gating window of 3 mm. The navigator triggers the spectroscopy sequence and tracks the position of the diaphragm updating the spectroscopy voxel location dynamically with respect to the actual position of the heart. The stability of the amplitude was determined by calculating the standard deviation of the signal for the three respiratory compensation methods. The variations of the center frequency and phase of the water signal were also determined. The amplitude variation, center frequency variation, and phase variations for the three different methods were compared using Friedman's test and post hoc Wilcoxon signed rank test.

Efficiency of Different Water Suppression Methods.
Three different water suppression techniques were assessed in eight subjects: frequency selective excitation,[19] Chemical Shift Selective (CHESS)[20,21] and Multiply Optimized Insensitive Suppression Train (MOIST) water suppression.[22] Frequency selective excitation water suppression uses two selective RF pulses combined with crusher gradients to minimize the water magnetization at the beginning of the acquisition. CHESS water suppression uses three narrowband chemical shift selective pulses, while MOIST water suppression uses four phase-modulated RF pulses, such that the longitudinal magnetization of the water signal is minimized at the beginning of the acquisition. Four non–water-suppressed averages and 16 water-suppressed averages were acquired for each subject. A residual water fraction was calculated by dividing the water signal in the suppressed spectrum by the water signal in the non–watersuppressed spectrum. A Friedman's test was performed to analyze differences in the residual water signal between the three water suppression techniques, and post hoc tests were performed with the Wilcoxon signed-rank test. Spectra were also visually inspected to assess spectral quality in terms of baseline distortion and the presence of spurious signals from incomplete water suppression.

Assessment of the Inter- and Intrasession Reproducibility of MTGC Quantification
Using the optimized parameters derived in the results section, spectra (6 averages without water suppression, 32 averages with water suppression) were acquired in eight subjects. The MTGC was calculated from the formula:

$$\text{MTGC} = \frac{\text{triglyceride methyl (CH}_3) + \text{triglyceride methylene (CH}_2)^n}{\text{water} + \text{triglyceride methyl (CH}_3) + \text{triglyceride methylene (CH}_2)^n} \times 100\% \quad \text{(Equation 1)}$$

The scan was then repeated and the MTGC of the two scans compared with determine the intrasession reproducibility. In seven of the eight cases (one was not possible due to a 1 h time limit on scanning), the subject was then fully removed from the scanner, positioned back on the patient bed, and the protocol was re-run to determine the intersession reproducibility. To determine the intersession reproducibility, spectra were compared with the first scan acquired. The coefficient of variation (C_v) was determined and the Spearman correlation coefficient was calculated to determine the intra- and intersession correlation and Bland-Altman plots were constructed.

Data Processing
All spectra were fitted in the time-domain using the Java-based MR User Interface (jMRUI).[23] The advanced method for accurate, robust and efficient spectral fitting (AMARES) algorithm was used to fit the resonances to a Gaussian line shape. The water and lipid SNRs were defined as the integrated area under the water peak and the sum of the integrated area under the triglyceride-methyl (CH$_3$) and the triglyceride-methylene (CH$_2$)^n peaks, divided by the standard deviation (SD) of the noise, respectively. The noise was taken from the last 100 points of the free induction decay.

Statistical Analysis
All statistical analyses were performed using the statistical software IBM SPSS Statistics (version 20, IBM, Chicago, IL). Plots were created using GraphPad Prism (GraphPad Software, San Diego, CA). Numerical data were reported as mean ± standard deviation. Data were considered statistically significant at P-values < 0.05.

RESULTS
POWER OPTIMIZATION

Figure 1 shows water-suppressed spectra acquired using global and local power optimizations in a male subject with a body mass index (BMI) of 30.3 kg/m^2. The SNR of the lipid increased from 17 to 38 arbitrary units (a.u.) using the local power optimization compared with the global power optimization. Figure 2 plots the SNR of the water signal for all 15 subjects. The spectra of 13 of the 15 subjects show a higher SNR using local power optimization compared with global power optimization, while for the remaining two subjects the SNR did not differ. The mean SNR (±SD) of the water signal was 1787 (±787) using global power optimization versus 2173 (±626) for local power optimization (P = 0.0002).

Global
Power Optimization

Lipid SNR = 17

Local
Power Optimization
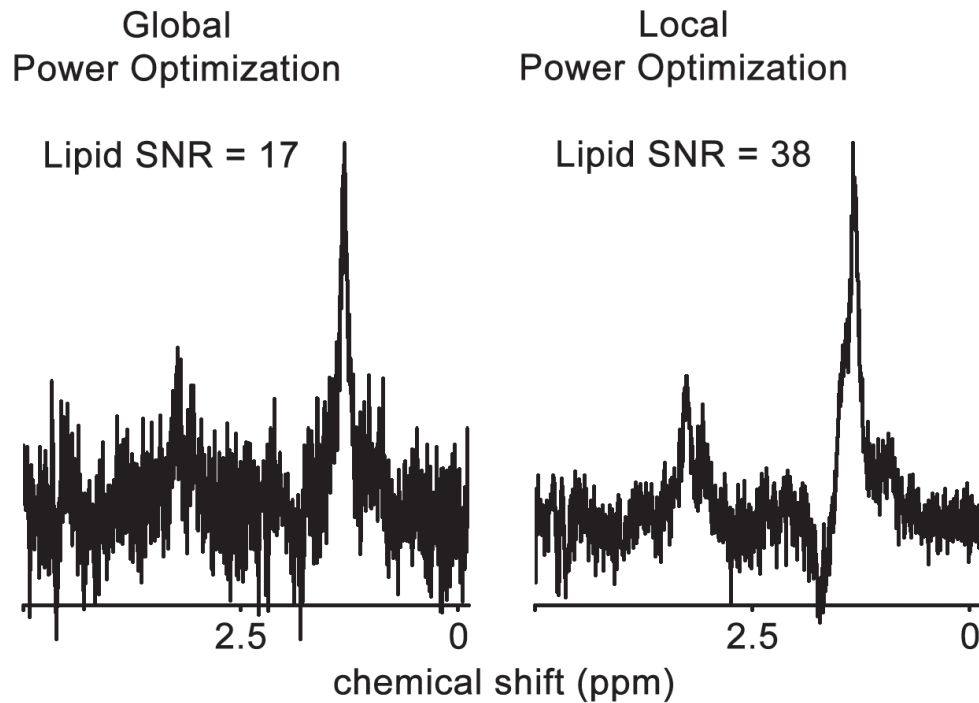
Lipid SNR = 38

chemical shift (ppm)

FIGURE 1: Cardiac MR spectrum acquired with global power optimization (left), a spectrum (right), in the same subject, is shown using local power optimization within the spectroscopic VOI.

COMPARISON OF SPECTRAL LINEWIDTHS FOR FREE-BREATHING AND BREATHHOLD B$_0$ SHIMMING

The mean linewidth after performing pencil-beam B$_0$ shimming during free-breathing was 19.1 Hz (±3.2 Hz) compared with 17.5 Hz (±4.6 Hz) when shimming was performed during breathholds: these values were not significantly different (P = 0.15). The mean of the standard deviation of the three successive linewidth measurements in each volunteer was 2.3 Hz (free-breathing) and 1.5 Hz (breathholds).
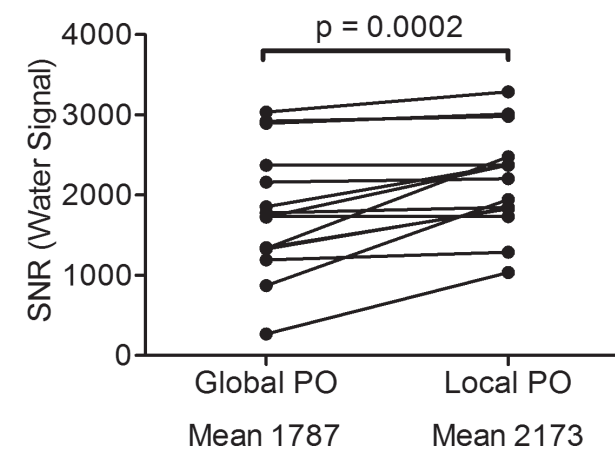
Power optimization method

p = 0.0002

FIGURE 2: SNR of the water signal for global- and local power optimization in 15 subjects. The spectra of 13 of the 15 subjects show a higher SNR using local power optimization compared with global power optimization, while for the remaining two subjects the SNR did not differ.

AMPLITUDE STABILITY AS A FUNCTION OF THE MEASUREMENT POINT WITHIN THE CARDIAC CYCLE

Figure 3 plots the standard deviation of the nonsuppressed water signal as a function of the cardiac trigger delay for three subjects. The average standard deviations were 0.18, 0.06, 0.07, 0.06, 0.22, 0.34, 0.15, and 0.15 for a cardiac trigger delay of 50, 150, 200, 250, 300, 500, and 700 ms, respectively. For all subjects, the SD had a minimum value, corresponding to the highest signal stability, at a trigger delay around 240 ms. This value agrees well with a previous study,[24] which is why only a relatively small number of subjects were used for this particular optimization step.

Subject 1, 46 bpm
Subject 2, 56 bpm
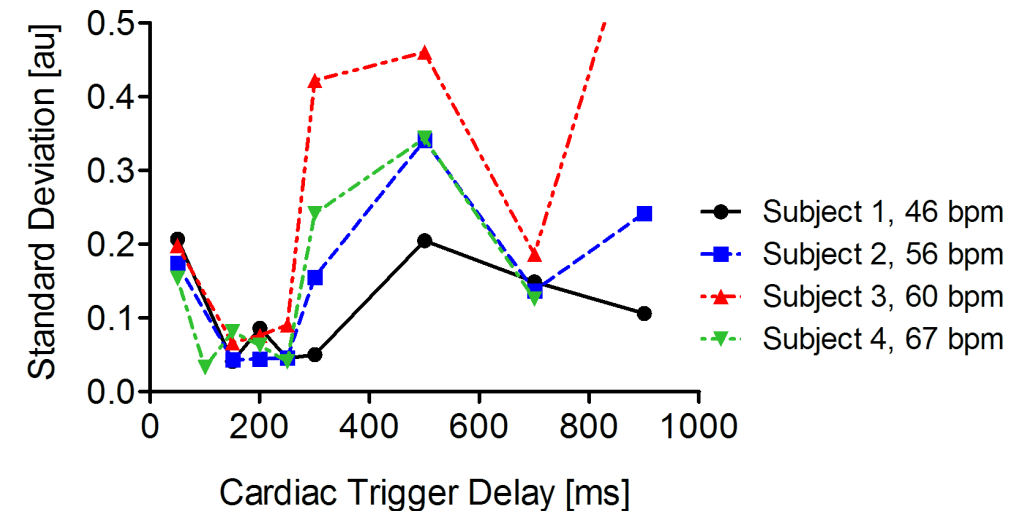Subject 3, 60 bpm
Subject 4, 67 bpm

FIGURE 3: Standard deviation of the water signal for eight measurement time points in the cardiac cycle. The lowest standard deviation and thus the most stable measurement point in the cardiac cycle is around 200 ms after the peak of the R-wave. The heart rate is shown in beats per minute (bpm).

COMPARISON OF SIGNAL REPRODUCIBILITY BETWEEN FREE-BREATHING, BREATH-HOLD, AND NAVIGATOR TRIGGERING

The mean variations of the amplitude (P = 0.001), frequency (P = 0.001) and phase (P = 0.016) of the water peak were significantly different for the three different breathing compensation methods (Figure 4). The mean amplitude variation was significantly lower for breathholds versus free-breathing (0.09 versus 0.22; P = 0.03) and for navigator triggering versus free-breathing (0.06 versus 0.22; P = 0.03), as well as for navigator triggering versus breathhold (0.06 versus 0.09; P = 0.02).

The mean variation of the water peak center frequency was 4.81 Hz (±5.18 Hz), 2.86 Hz (±2.82 Hz), and 1.37 Hz (±0.71 Hz) using free-breathing, breathholds, and navigator triggering, respectively (P = 0.008). The center frequency variation was significantly lower for breathholds versus free-breathing (P = 0.05) and for navigator triggering versus free-breathing (P = 0.02). The mean (SD) variation of the signal phase was 0.22 radians (±0.07 radians), 0.13 radians (±0.05 radians), and 0.12 radians (±0.02 radians) using free-breathing, breathholds, and navigator triggering, respectively (P = 0.016). The center frequency variation was significantly lower for breathholds versus free-breathing (P = 0.05) and for navigator triggering versus freebreathing (P = 0.02).
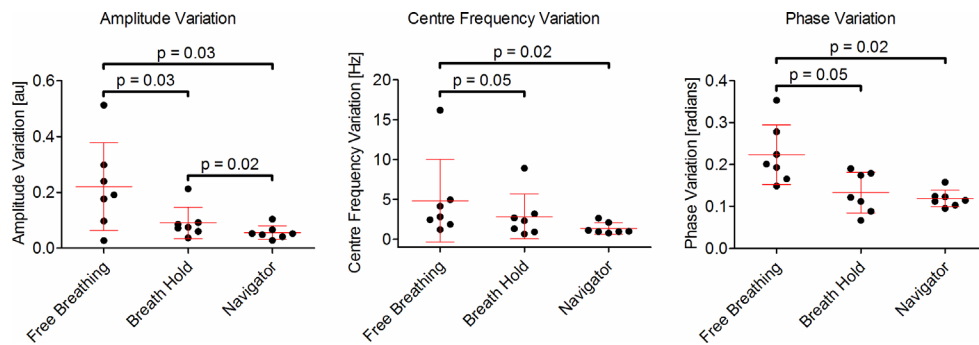
FIGURE 4: Variations in the amplitude, center frequency, and phase of the water signal over 16 acquisitions for free-breathing and two methods of motion compensation. The Friedman's test showed significant differences for the amplitude variation (P = 0.001) (left), center frequency variation (P = 0.001) (middle), and phase variation (P = 0.016) (right). Post hoc tests showed that variations in the mean amplitude, center frequency and phase were significantly different between free-breathing versus breathholds as well as between free-breathing versus navigator triggering. The mean of the amplitude variation was also significantly different between breathholds and navigator triggering.

EFFICIENCY OF WATER-SUPPRESSION METHODS

Figure 5 shows three water-suppressed spectra with the three different suppression techniques in the same subject. The Friedman's test showed significant differences in the residual water signal for frequency selective excitation, CHESS, and MOIST water suppression techniques (P = 0.001). Figure 6 shows the results from all subjects. The mean residual water signal was 7.0% (4.8%) using frequency-selective excitation, 1.1% (0.9%) using CHESS water-suppression, and 0.7% (0.4%) using the MOIST technique. Both the MOIST (P = 0.01) and CHESS (P = 0.01) techniques gave significantly lower residual water signals than the frequency selective excitation sequence, but there was no statistical significance between MOIST and CHESS (P = 0.46).

Due to the poor suppression the selective excitation sequence often introduced a significant baseline distortion in the spectrum, making MTGC quantification more difficult. In terms of choosing between the CHESS and MOIST techniques, the CHESS sequence is relatively long, requiring an increase in the suppression bandwidth to 240 Hz to be able to use a cardiac trigger delay of 200 ms. The length of the MOIST sequence is less than that of CHESS, requiring a lower suppression bandwidth of 190 Hz for a trigger delay of 200 ms. Given this, and the slightly higher degree of water suppression, the MOIST sequence was used for MTGC quantitation.
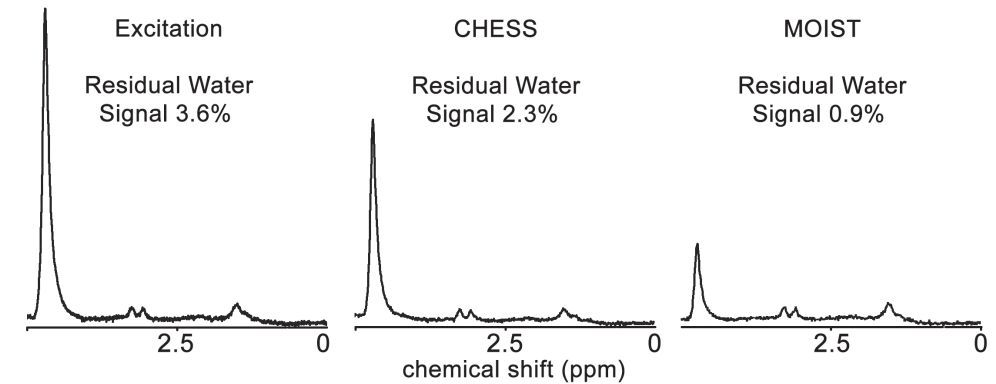
FIGURE 5: Water-suppressed spectra using three different water suppression techniques in the same subject. The residual water signal was calculated by dividing the water peak amplitude from the suppressed spectrum by that in the unsuppressed spectrum.
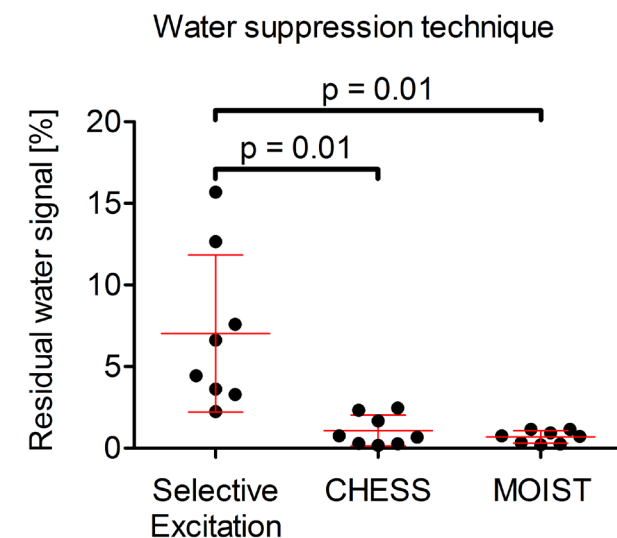
FIGURE 6: Residual water signal for the three different water suppression techniques for all the subjects studied. The residual signals for frequency selective excitation and CHESS water suppression were significantly different, as were those for frequency selective excitation and MOIST water suppression.

ASSESSMENT OF THE INTER- AND INTRASESSION REPRODUCIBILITY OF MTGC QUANTITATION

Figure 7 shows three spectra acquired from the same volunteer using the optimized scan parameters determined in the previous sections. The spectra on the left and center of Figure 7 were acquired in a single scan session to determine the intrasession reproducibility. The spectrum on the right was acquired in a separate scan session to determine the intersession reproducibility. The mean (±SD) MTGC of the intrasessions (n = 8) was 0.55% (±0.40%) and 0.59% (±0.42%), with a correlation coefficient r = 1.000 (P < 0.0001). The coefficient of variation for the intrasession reproducibility was 5% and the Bland-Altman analysis showed a mean difference of 0.04% with limits of agreement from -0.11% to +0.04% (Figure 8A). The mean (±SD) MTGC of the intersessions (n = 7) was 0.60% (±0.42%) and 0.63% (±0.45%) with a correlation coefficient r = 1.000 (P = 0.0004). The coefficient of variation for the intersession reproducibility was 6.5% and the Bland-Altman analysis showed a difference of 0.03% and limits of agreement from -0.15% to +0.9% (Figure 8B).
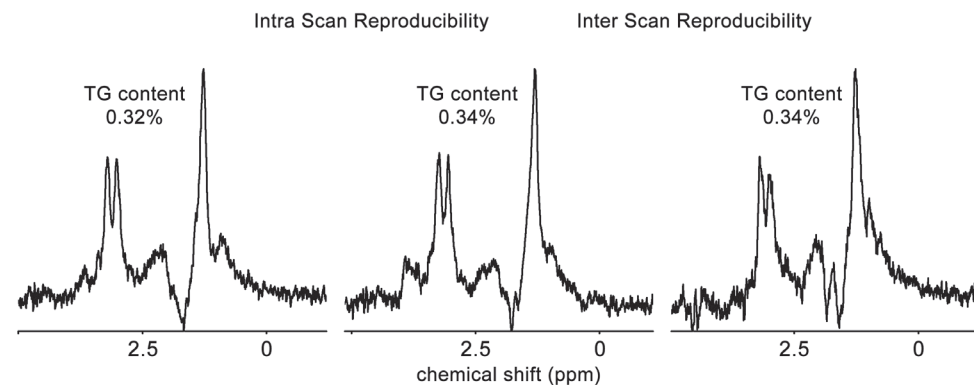

FIGURE 7: Left and center: Two spectra acquired successively are shown to calculate the intrasession reproducibility. Right: A spectrum from the same volunteer acquired in a different scanning session to assess the intersession reproducibility.
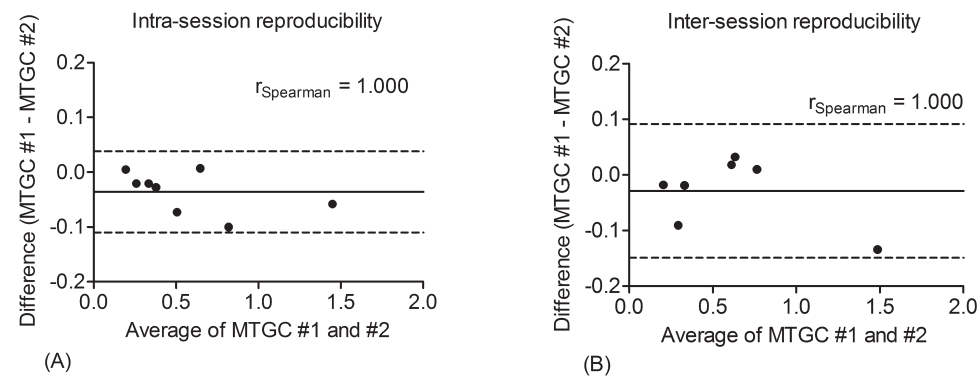

FIGURE 8: Bland-Altman plots for both intra- and intersession reproducibility. The Spearman correlation coefficient was 1.000 for both the intersession **(left)** and intrasession **(right)** measurements. The intrasession reproducibility mean difference was 0.04% with limits of agreement from -0.11% to +0.04%. The intersession reproducibility mean difference was 0.03% with limits of agreement from -0.15% to +0.9%.

DISCUSSION

This study looked at the effect of several different data acquisition parameters with the aim of being able to perform reproducible cardiac proton spectroscopy on a clinical 3 T platform. In terms of SNR, using local rather than global power optimization showed a significant increase. Indeed, from the 15 subjects studied there were five cases that resulted in a SNR gain of 35% or more which is in line with a prior study.[25] Local power optimization requires no changes to the system software, and so is easy to implement in a clinical setting. We observed that the power underestimation from a global power measurement was greatest in subjects with either high BMI or athletic subjects with high lung volume, but further study would be required to confirm this observation.

With respect to spectral quality, i.e., linewidth and lineshape, there was no statistical difference between performing B_0 shimming during free-breathing or breathholds. In this study we did not compare image-based shimming to the pencil beam technique because the former technique is not implemented on most clinical systems. In the future, this would be interesting to investigate because image-based shimming is generally more robust and gives improved linewidths in cardiac imaging.[25]

With respect to spectral reproducibility (and SNR because individual spectra are co-added in signal averaging), the key parameters are the measurement point within the cardiac cycle, and the form of motion compensation used. In previous publications some authors have measured in systole and others in the diastolic phase.[8,9,16,26] The results in this study show that the beginning of the systolic heart phase (200–250 ms after the peak of the R-wave) has the highest stability: this agrees well with the findings of a previous study.[24] Given that the range of heart rates was not extensive (range, 46–67 bpm) the optimal measurement point was only minimally affected by the heart rate for these subjects, which can be explained by the small influence of the heart rate on the length of the systolic heart phase.[27]

In another study of Weiss et al, it was shown that the maximum SNR in cardiac spectroscopy was achieved in midsystole with a trigger delay < 300 ms. However, mid-systole is relatively close to the point that the stability of the signal decreases strongly.[28] In that study, they also propose an improved spectroscopy sequence to decrease the sensitivity of the sequence to cardiac motion, using very strong crusher gradients. In earlier studies, it was also shown that respiratory compensation should be used to increase the reproducibility of cardiac MRS.[13,29,30] Our results show that, by using breathholds, it is possible to increase the signal stability significantly. However, the navigator-based respiratory compensation resulted in significantly lower variations in signal intensity and signal frequency/phase than using breathholds. In addition, many classes of patients have problems maintaining breathholds for prolonged periods of time. Therefore, the navigator-based respiratory compensation is preferred over breathhold.

With respect to water suppression, the CHESS and MOIST techniques both showed suppression ratios of approximately 100:1, with MOIST giving slightly better water suppression and more consistent results. However, MOIST is a manufacturer specific variant on the CHESS sequence in terms of parameter optimization. Because no statistical difference was measured between the two techniques, the more standard CHESS sequence may be able to be substituted where necessary.

Using the optimized protocol proposed in this study, it was possible to get an intersession reproducibility of the MTGC of 6.5% which is in line with the findings of Ith et al.[31] It should be noted that in that study the creatine signal was used as a reference whereas in our

current study we used the water signal. The reproducibility reported here is also much higher than other studies performed at 1.5 T. For example, it was shown by Felblinger et al that, by using the ECG electrodes to measure the respiratory phase while an optical ECG sensor was used to measure the cardiac cycle, it was possible to get an intersession coefficient of variation of 13%. Szczepaniak et al showed that using a respiratory pressure belt and ECG triggering it was possible to get an intersession coefficient of variation of 17%.[30] In van der Meer et al, the coefficient of variation was 17.9% using navigator-based respiratory compensation.[8] With the optimized protocol proposed in this study the limits of agreement for the Bland Altman analysis lay between −0.15% and +0.9% compared with −0.14 and +0.19 for the study performed by van der Meer et al.

In terms of study limitations, one is that we have only provided optimized parameters for the measurement location in the myocardial septum, which is a relevant region for studying the effects of metabolic syndrome and type 2 diabetes mellitus but not for localized tissue changes such as myocardial infarcts. In this study, the total group of volunteers was relatively large: however, because there were multiple topics of interest the sample size for each individual topic were smaller. We also note that this study was performed on healthy subjects where the efficiency of the navigator is high (around 50%) but some patients tend to have irregular breathing patterns that will most likely result in decreased navigator efficiency and increased scan time.

In conclusion, using the optimized protocol with local power optimization, pencil beam B0 shimming, a cardiac trigger delay of 200 ms, pencil beam navigator-based respiratory compensation, and MOIST water suppression, we were able to achieve an high intra- and intersession reproducibility of the MTGC. The preparation time of the spectroscopy scan was 1 min and 3 s (power optimization 3 s, resonance frequency determination 24 s, and pencil beam B0 shimming 36 s), and the acquisition of the spectra (4 unsuppressed averages and 32 suppressed averages) was 4 min and 24 s with an navigator efficiency of 50%. This resulted in an average total scan time of 5.5 min.

ACKNOWLEDGMENTS

REFERENCES

1. Kankaanpaa M, Lehto HR, Parkka JP, et al. Myocardial triglyceride content and epicardial fat mass in human obesity: relationship to left ventricular function and serum free fatty acid levels. J Clin Endocrinol Metab 2006;91:4689–4695.

2. McGavock JM, Lingvay I, Zib I, et al. Cardiac steatosis in diabetes mellitus: a 1H-magnetic resonance spectroscopy study. Circulation 2007;116:1170–1175.

3. Bizino MB, Hammer S, Lamb HJ. Metabolic imaging of the human heart: clinical application of magnetic resonance spectroscopy. Heart 2014;100:881–890.

4. Singerman RW, Denison TJ, Wen H, Balaban RS. Simulation of B1 field distribution and intrinsic signal-to-noise in cardiac MRI as a function of static magnetic field. J Magn Reson 1997;125:72–83.

5. Sung K, Nayak KS. Measurement and characterization of RF nonuniformity over the heart at 3T using body coil transmission. J Magn Reson Imaging 2008;27:643–648.

6. Greenman RL, Shirosky JE, Mulkern RV, Rofsky NM. Double inversion black-blood fast spin-echo imaging of the human heart: a comparison between 1.5T and 3.0T. J Magn Reson Imaging 2003;17:648–655.

7. Gutberlet M, Noeske R, Schwinge K, Freyhardt P, Felix R, Niendorf T. Comprehensive cardiac magnetic resonance imaging at 3.0 Tesla: feasibility and implications for clinical applications. Invest Radiol 2006; 41:154–167.

8. van der Meer RW, Doornbos J, Kozerke S, et al. Metabolic imaging of myocardial triglyceride content: reproducibility of 1H MR spectroscopy with respiratory navigator gating in volunteers. Radiology 2007; 245:251–257.

9. Rial B, Robson MD, Neubauer S, Schneider JE. Rapid quantification of myocardial lipid content in humans using single breath-hold 1H MRS at 3 Tesla. Magn Reson Med 2011;66:619–624.

10. Bilet L, van de Weijer T, Hesselink MKC, et al. Exercise-induced modulation of cardiac lipid content in healthy lean young men. Basic Res Cardiol 2011;106:307–315.

11. Jonker JT, Snel M, Hammer S, et al. Sustained cardiac remodeling after a short-term very low calorie diet in type 2 diabetes mellitus patients. Int J Cardiovasc Imaging 2014;30:121–127.

12. Clayton DB, Elliott MA, Leigh JS, Lenkinski RE. 1H Spectroscopy without solvent suppression: characteriza-tion of signal modulations at short echo times. J Magn Reson 2001;153:203–209.

13. Schar M, Kozerke S, Boesiger P. Navigator gating and volume tracking for double-triggered cardiac proton spectroscopy at 3 Tesla. Magn Reson Med 2004;51:1091–1095.

14. Nakae I, Mitsunami K, Omura T, et al. Proton magnetic resonance spectroscopy can detect creatine depletion associated with the progression of heart failure in cardiomyopathy. J Am Coll Cardiol 2003; 42:1587–1593.

15. Reingold JS, McGavock JM, Kaka S, Tillery T, Victor RG, Szczepaniak LS. Determination of triglyceride in the human myocardium by magnetic resonance spectroscopy: reproducibility and sensitivity of the method. Am J Physiol Endocrinol Metab 2005;289:E935–E939.

16. Weiss K, Martini N, Boesiger P, Kozerke S. Cardiac proton spectroscopy using large coil arrays. NMR Biomed 2013;26:276–284.

17. Frahm J, Merboldt KD, Hanicke W. Localized proton spectroscopy using stimulated echoes. J Magn Reson (1969) 1987;72:502–508.

18. de Heer P, Bizino MB, Versluis MJ, Webb AG, Lamb HJ. Improved cardiac proton magnetic resonance spectroscopy at 3 T using high permittivity pads. Invest Radiol 2015;51:134–138.

19. Morris GA, Freeman R. Selective excitation in Fourier transform nuclear magnetic resonance. 1978. J Magn Reson 2011;213:214–243.

20. Haase A, Frahm J, Hanicke W, Matthaei D. 1H NMR chemical shift selective (CHESS) imaging. Phys Med Biol 1985;30:341–344.

21. Ogg RJ, Kingsley PB, Taylor JS. WET, a T1- and B1-insensitive watersuppression method for in vivo localized 1H NMR spectroscopy. J Magn Reson B 1994;104:1–10.

22. Murdoch JB, Lampman DA. Beyond WET and DRY: optimized pulses for water suppression. In: Proceedings of the 12th Annual Meeting of SMRM, New York, 1993. (abstract 1191).

23. Naressi A, Couturier C, Devos JM, et al. Java-based graphical user interface for the MRUI quantitation package. MAGMA 2001;12:141–152.

24. A°sa Carlsson, Maja Sohlin, Maria Ljungberg, Eva Forssell-Aronsson. The cardiac triggering time delay is decisive for the spectrum quality in cardiac 1H MR Spectroscopy. In: Proceedings of the 20th Annual Meeting of ISMRM, Melbourne, 2012. (abstract 1793).

25. Sch€ar M, Vonken EJ, Stuber M. Simultaneous B0- and B11-Map acquisition for fast localized shim, frequency, and RF power determination in the heart at 3 T. Magn Reson Med 2010;63:419–426.

26. Venkatesh BA, Lima JA, Bluemke DA, Lai S, Steenber-gen C, Liu CY. MR proton spectroscopy for myocardial lipid deposition quantification: a quantitative comparison between 1.5T and 3T. J Magn Reson Imaging 2012;36:1222–1230.

27. Boron WF, Boulpaep EL. Medical physiology. 2nd ed. Philadelphia, PA: Saunders/Elsevier; 2009.

28. Weiss K, Summermatter S, Stoeck CT, Kozerke S. Compensation of signal loss due to cardiac motion in point-resolved spectroscopy of the heart. Magn Reson Med 2014;72:1201–1207.

29. Felblinger J, Jung B, Slotboom J, Boesch C, Kreis R. Methods and reproducibility of cardiac/respiratory double-triggered (1)H-MR spectroscopy of the human heart. Magn Reson Med 1999;42:903–910.

30. Szczepaniak LS, Dobbins RL, Metzger GJ, et al. Myocardial triglycerides and systolic function in humans: in vivo evaluation by localized proton spectroscopy and cardiac imaging. Magn Reson Med 2003;49: 417–423.

31. Ith M, Stettler C, Xu J, Boesch C, Kreis R. Cardiac lipid levels show diurnal changes and long-term variations in healthy human subjects. NMR Biomed 2014;27:1285–1292.